NASA TECHNICAL NOTE

NASA TN D-2995

NASA TN D-2995

DEVELOPMENT AND TESTING OF A PROPOSED INFRARED HORIZON SCANNER FOR USE IN SPACECRAFT ATTITUDE DETERMINATION

by Norman M. Hatcher, Arthur L. Newcomb, Jr., and Nelson J. Groom

Langley Research Center
Langley Station, Hampton, Va.

NATIONAL AERONAUTICS AND SPACE ADMINISTRATION • WASHINGTON, D. C. • SEPTEMBER 1965

NASA TN D-2995

DEVELOPMENT AND TESTING OF A PROPOSED INFRARED HORIZON SCANNER FOR USE IN SPACECRAFT ATTITUDE DETERMINATION

By Norman M. Hatcher, Arthur L. Newcomb, Jr., and Nelson J. Groom

Langley Research Center
Langley Station, Hampton, Va.

NATIONAL AERONAUTICS AND SPACE ADMINISTRATION

For sale by the Clearinghouse for Federal Scientific and Technical Information
Springfield, Virginia 22151 – Price $2.00

DEVELOPMENT AND TESTING OF A PROPOSED INFRARED HORIZON SCANNER FOR USE IN SPACECRAFT ATTITUDE DETERMINATION

By Norman M. Hatcher, Arthur L. Newcomb, Jr.,
and Nelson J. Groom
Langley Research Center

SUMMARY

33844

An attitude sensing horizon scanner for spacecraft that detects the thermal radiation discontinuity at opposite horizons of a planetary body to determine spacecraft attitude has been designed. An experimental model, incorporating many of the features of the proposed scanner, has been constructed and used for testing purposes. Results of tests with the experimental model indicate that the proposed scanner could perform as predicted earlier in a theoretical report (NASA Technical Note D-1005) on the scanner design. That is, it would have an instrument-associated error of less than 0.1°, a signal-to-noise ratio that would allow it to operate at altitudes of about a million miles from the earth, a power consumption rate of about 3.5 watts, the ability to reject signals from the sun, and a wide-angle capture capability.

An alternate solenoid-type scanning-mirror drive mechanism for the scanner has been examined. Laboratory tests with an experimental model of the drive system indicate that it could be effectively used to further increase lifetime while decreasing weight, volume, and power consumption.

Author

INTRODUCTION

With the evolution of spacecraft toward greater refinement of operation and longer operational lifetimes, the requirements upon moon- or planet-seeking attitude sensors, or scanners, as these sensors will be referred to in this report, are becoming more stringent. For example, reliable operation, accuracy, low power consumption, small size, low weight, and the ability to discriminate against radiation sources other than the desired target are generally required of all scanners, while operational lifetime of a year or more, wide-angle capture capability, or the ability to easily sense spacecraft altitude in addition to attitude may be required of some scanners.

The existing scanners that contain moving parts seem to impose greater physical demands upon the spacecraft than necessary and, in general, friction levels of their scanning mechanisms are so high that they could only operate for short periods of time in space. Efforts to increase operational lifetime

through the complete elimination of moving parts have usually resulted in even greater electronic complexity, degraded accuracy, or excessive volume, weight, and power consumption.

It is therefore believed that a need exists for a versatile scanner that imposes relatively minor requirements upon the spacecraft and one which is nevertheless accurate and simple enough in operation and construction to be reliable and capable of operating for periods of a year or more in space. The scanner discussed in this report has been designed with the goal of incorporating as many of the abovementioned desirable features as possible. Ground-based performance tests on a laboratory test model of the scanner indicate that most of these features can be incorporated in a single instrument.

The basic operating principles of the scanner and its optical geometry are described in reference 1. The present report describes certain modifications that have been made to the proposed scanner since reference 1 was written; it explains in detail the scanner electronics which had not been developed at the time of the earlier report; it gives results of several ground-based performance tests that have been conducted on the laboratory test model; and it suggests a means of probable further improvement to the scanner through the incorporation of a unique scanning-mirror drive system.

PRINCIPLES OF OPERATION

The scanner makes use of the discontinuity in emitted infrared radiation which exists between space and the lunar or planetary target to determine the direction toward the center of the target. It contains four thermistor infrared radiation detectors whose fields of view are rotated in two perpendicular planes from space across the horizon, or edges, of the planetary body as shown in figure 1. The two detector fields of view in each plane are rotated synchronously; that is, at any instant during their scan cycle the two fields make equal angles with the principal axis of the scanner. Thus, if the scanner is oriented toward the center of the planetary body, the fields of view of the two detectors in each plane will cross the planetary horizons simultaneously. The influx of infrared radiation will cause each detector to produce an output simultaneously and these outputs will be processed by the electronic system to indicate correct attitude. However, if a pointing error exists, as in figure 1, the field of view of one detector will cross one horizon before the field of view of the second detector in the same scanning plane crosses the opposite horizon. Since the scanning rate is constant, the time difference between crossing opposite horizons in one scanning plane is directly proportional to pointing error in this plane. The direction of pointing error is determined by noting which of the detectors first detects the radiation discontinuity.

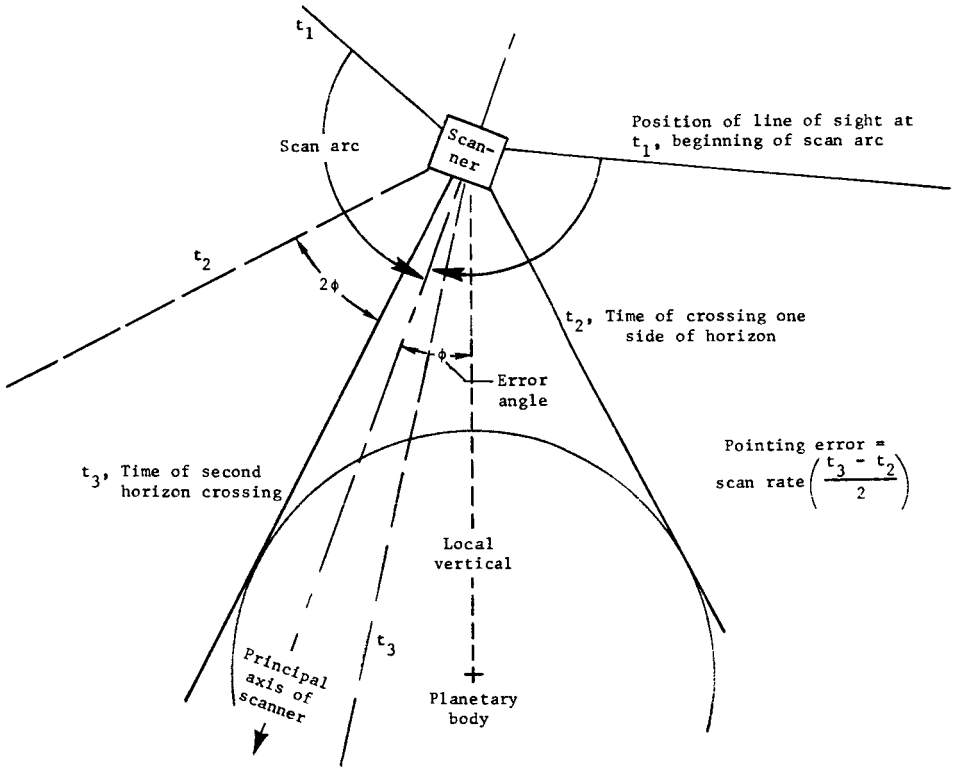

Figure 1.- Attitude determination.

DISCUSSION OF SCANNER DESIGN

Optical and Mechanical System

Figure 2 shows the optical system of the scanner and figure 3 shows the assembled configuration. The optics consists of four germanium lenses, four parabolic reflector segments, and four flat mirrors rotated by a slow-speed motor mounted above the optics. (An alternate mirror drive system is described in appendix A.) As the mirrors are rotated, the fields of view of the detectors are caused to scan through arcs from space across the horizons of the planetary body. Incoming radiation is reflected from the rotating mirrors to the parabolic reflector segments which, in turn, reflect and converge the radiation upon the germanium lenses. The lenses focus the radiation upon thermistor detectors attached to the rear surfaces of the lenses. Thermistors attached to germanium lenses in this manner are called immersed thermistors and offer a responsivity (voltage output/radiation input) gain over nonimmersed detectors of about 3.5 (ref. 2). Also, the lenses function as filters for removing radiation with wavelengths below 1.8 microns and thus eliminate most of the unwanted direct and reflected radiation from the sun.

As shown in figure 2 the two mirrors in one plane are made to rotate 90° out of phase with the mirrors in the second plane. This phase relation is maintained as they are driven by an intermeshing gear set. The flat mirrors are faced on both sides which allows them to make two scans per revolution. The

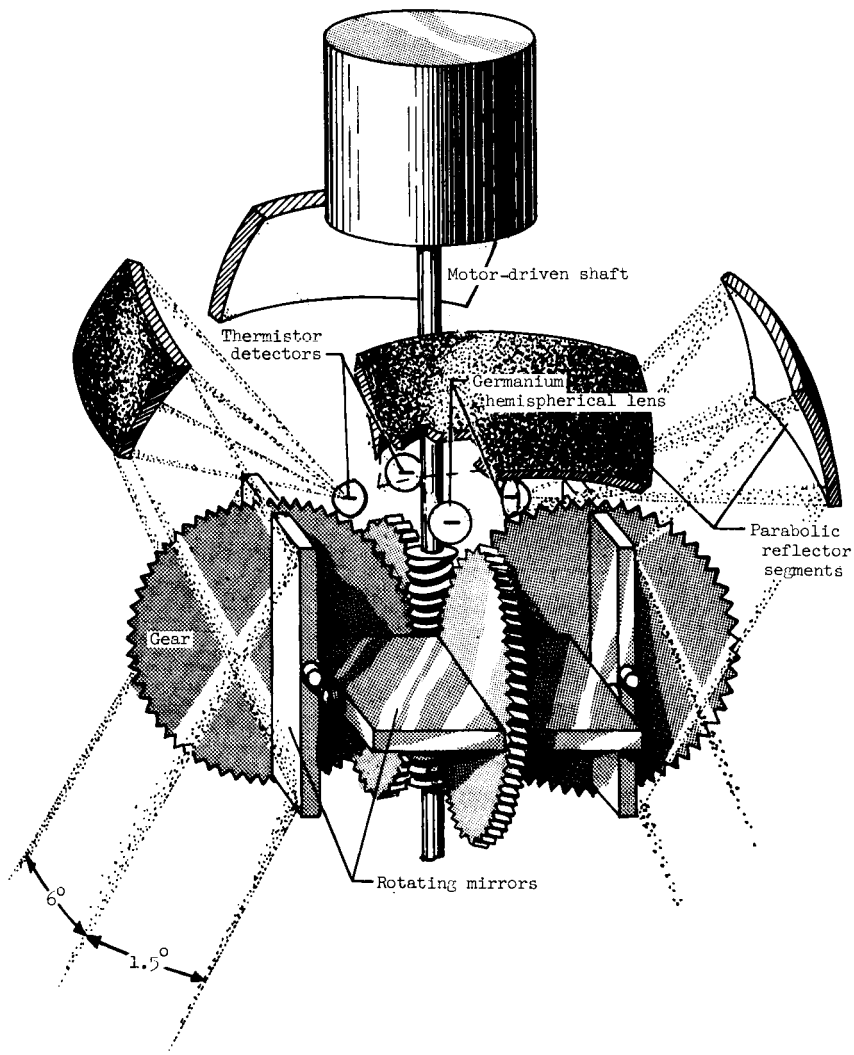

Figure 2.- Optical system and mirror drive mechanism.

scan cycle of the mirrors in the two perpendicular planes are therefore separated by 90° of mirror rotation or 180° of scanning. This arrangement permits a compact optical system, requires only one mirror drive motor, and simplifies the gearing system.

In choosing a mirror drive system for the scanner, the achievement of low friction and thus long and reliable operating lifetimes has been sought. Although certain bearings with special lubricants have been operated continuously in a hard vacuum at 8000 rpm for over 1 year (ref. 3), the long-term usefulness of such bearings in space has not yet been completely verified. Thus the mirror drive system shown in figure 2 uses a low-speed (about 500 rpm) motor to rotate a steel helical gear which, in turn, rotates plastic gears encircling the flat mirrors at a rate of about 60 rpm. Most studies indicate that plastic gears, which were chosen here to prevent cold welding, will not deteriorate appreciably in the space vacuum (ref. 4). A suitable motor using from 1.5 to 2.0 watts can be obtained for the purpose of rotating the gears. Because of the relatively

slow speeds at which these parts rotate, this drive system is expected to be capable of operating for comparatively long times in space. Since operational lifetimes of several years will be required for certain missions, however, the possibility of incorporating a non-conventional low-friction drive system which might permit such lifetimes was investigated. One such system which appears promising is the electromagnetic drive system described in appendix A.

The pinion gear drive suggested in reference 1 is no longer recommended because space limitations within the scanner would dictate the use of a very small (size 8) motor which cannot be obtained with speeds lower than about 4200 rpm.

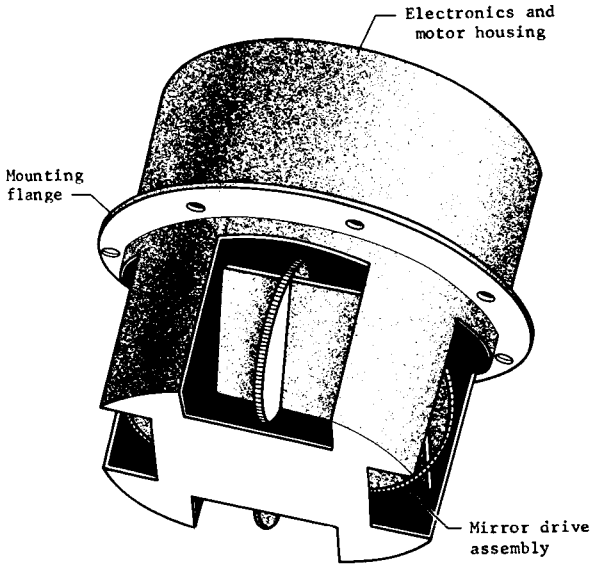

Figure 3.- Assembled configuration of proposed scanner.

Electronics

The main function of the scanner electronics is to convert the optical input to the thermistor detectors to an electrical output signal which indicates the direction and magnitude of vehicle pointing error. The electronics consists basically of the infrared sensing elements, the sensor preamplifiers, the time-difference detectors (TDD), and a conversion circuit, as shown in the block diagram of figure 4. The character of the signals at various points in the system is shown in figure 5. Details of the electronics used in the experimental scanner are discussed in appendix B. Time sharing of this circuitry by the detectors in the two scanning planes could be accomplished by the switching circuitry described in reference 1. However, this time-sharing scheme has been abandoned for the sake of reliability, and circuits identical to those shown in figure 4 will be required for signal processing in the second plane.

Infrared detector circuit.- A change in the amount of intercepted infrared radiation produced by scanning across the horizon is converted to an electrical signal in the thermistor detector bridge which contains optically shielded compensating elements. These compensators are of the same material as the active sensors and provide compensation for ambient temperature changes.

Sensor preamplifiers.- Outputs from the sensor bridge circuits are amplified by medium-high gain amplifiers. These amplifiers provide sufficient pulse outputs to trigger the TDD circuit, and the sun-signal-eliminator circuit when solar interference occurs.

The amplifier is of basic class A design. Fundamental requirements are that the amplifier have a stable gain over the required temperature range (about

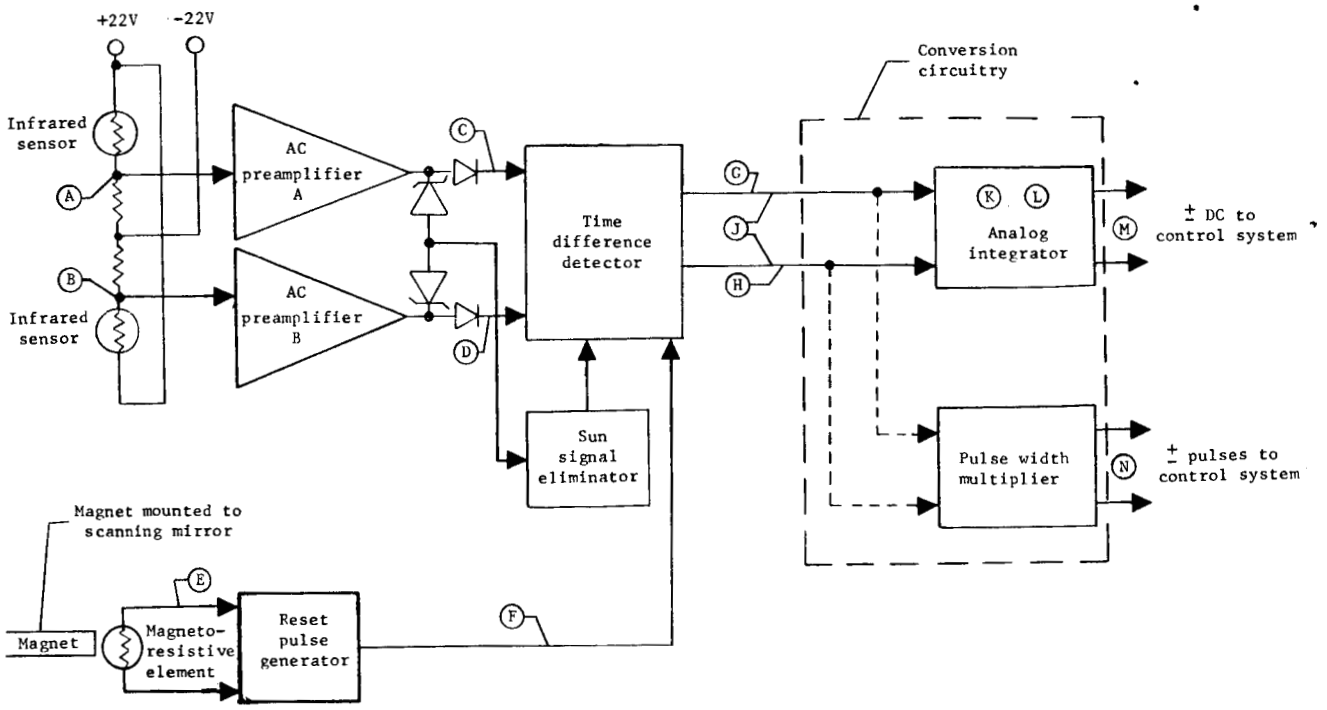

Figure 4.- Horizon scanner electronics block diagram. (One axis is shown.) Circled letters are points where waveforms of figure 5 are taken.

-25° C to 100° C) and have a response of about ±3 dB from 20 to 10,000 cycles per second.

Time-difference detector and reset pulse generator.- The time-difference detector (TDD) detects any difference in time between pulses from the two sensor preamplifiers, as when an attitude error exists. The TDD consists essentially of two silicon controlled switches (SCS) which are triggered by the amplified detector outputs as the horizons are crossed. The SCS's are connected so that their outputs subtract. Since the SCS outputs are of equal magnitude, a square-wave pulse of uniform height and of width equal to the time difference between crossing opposite sides of the horizon is produced. This, then, is the basic attitude error pulse. The direction of pointing error is determined by noting which of the two detectors first intercepts a horizon. The pulse can be integrated to provide a dc level or multiplied in width to accommodate a variety of spacecraft control systems.

The TDD is made to be monostable by a reset pulse generated at the beginning of the active portion of the scan cycle, or that portion during which the circuitry is sensitive to radiation inputs. This reset pulse is negative and of sufficient magnitude and time duration to clear the TDD circuitry of conduction currents.

The TDD reset pulse is generated by a magnetoresistive element which is appropriately placed in the scanner head to produce an output when a magnet of high flux density, attached to one of the scanning mirrors, passes by it. By

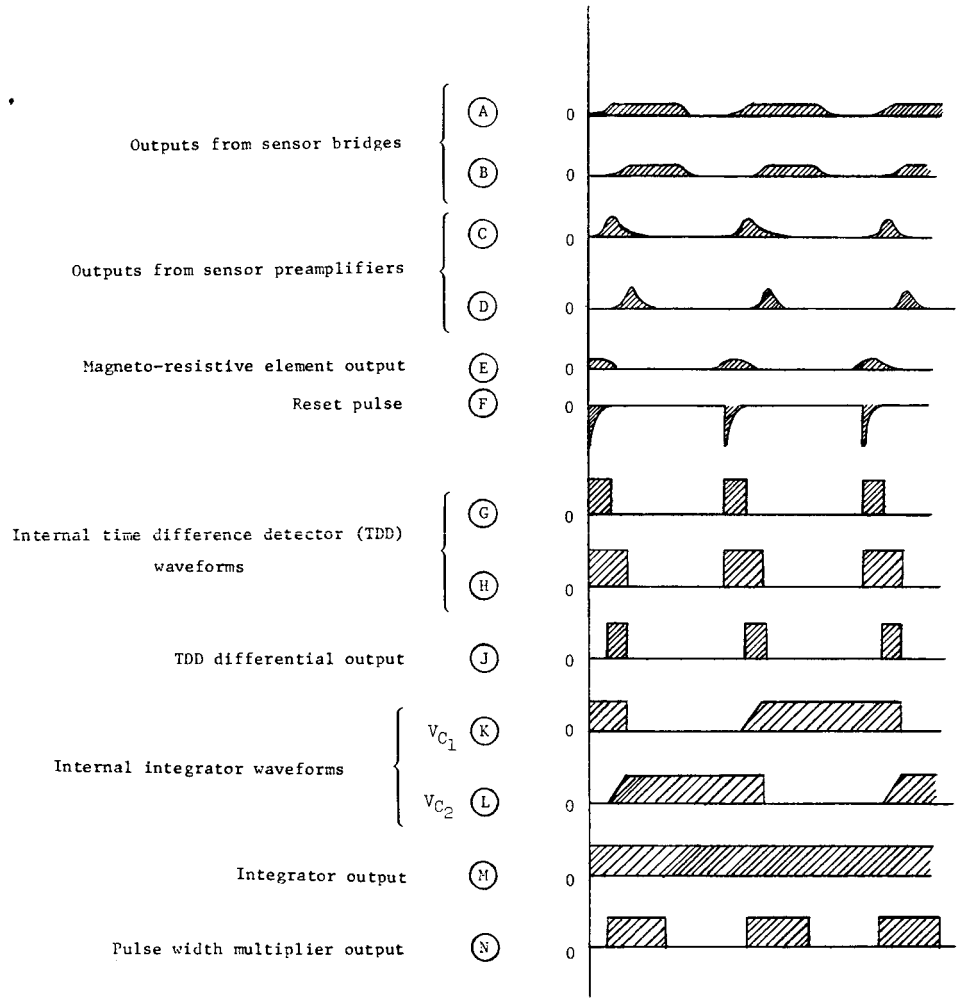

Figure 5.- Synchrogram of circuit waveforms.

adjusting the position of the magnetoresistive element, the active portion of the scan arc can be made to begin when the detector fields of view are at any desired angular position below about 30° above horizontal, with respect to the scanner. The circuitry then remains sensitive to any radiation input until horizon crossing occurs. Signals that are subsequent to the horizon crossover signal are not processed. Thus the active portion of the scan cycle is not terminated at some prescribed time, but rather at the time the TDD is triggered on upon crossing a planetary horizon.

The magnetoresistive element was chosen for its relative insensitivity to extraneous magnetic fields. The inductive pickup, proposed in reference 1, was found to be sensitive to both the motor field and other nearby magnetic disturbances. Since the magnetoresistive element has almost no inductance and is a low-impedance device (5000 Ω) it will only respond to extremely intense magnetic fields such as the field produced by an Alnico 5 magnet attached to a scanning mirror.

Conversion circuitry.- The output from the time-difference detector cannot be used directly because at small pointing-error angles where accurate attitude

information is most desirous and control most critical, the pulse is very narrow. For example, a pointing-error angle of 0.2° corresponds to a pulse width of only 1 millisecond. Therefore, it is necessary to modify this pulse somehow to make it usable with typical control systems. Two conversion circuits were investigated for this purpose - an analog and a pulse system.

The analog concept converts the attitude error pulse from the TDD to a dc voltage which has a magnitude indicative of the pulse width and a polarity the same as that of the pulse. The analog circuit (integrator) used in the experimental scanner consists of two capacitors, C_1 and C_2, which are alternately charged and read. While one capacitor is being charged, the other is being read through a high input-impedance circuit. The dc output voltage can then be fed to a control system as shown in figure 6 through a passive circuit lead network (ref. 5). This circuit is designed so that it provides the necessary vehicular rate detection for the particular control system used. If the analog output voltage of the scanner decreases at a rate faster than the discharge rate of the capacitor, the voltage to the control circuit reverses polarity, thereby actuating the opposite vehicular torquing device. System damping is controlled by varying the RC product of this circuit.

This circuit provides fast reaction time with an output which is updated every cycle and accurate to the most recent error pulse. This capability makes it possible to use the output as a rate signal since the change in output voltage is as close to vehicular rate as the scan rate allows. The saturation angle (vehicular error angle where maximum linear output is reached) can be set at any desired point up to about 60° pointing error. Laboratory experiments have shown that a compatible saturation angle can probably be chosen to satisfy both capture and hold requirements. Operation of the scanner is such that maximum error indication in one scanning plane is given in the proper direction even though only one sensor in this plane is able to "see" the target source.

The pulse concept uses a pulse-width multiplier which multiplies the TDD pulse width by a fixed factor that can be adjusted from approximately 5 to 50. This pulse can then be fed directly to the control torquers after proper power amplification.

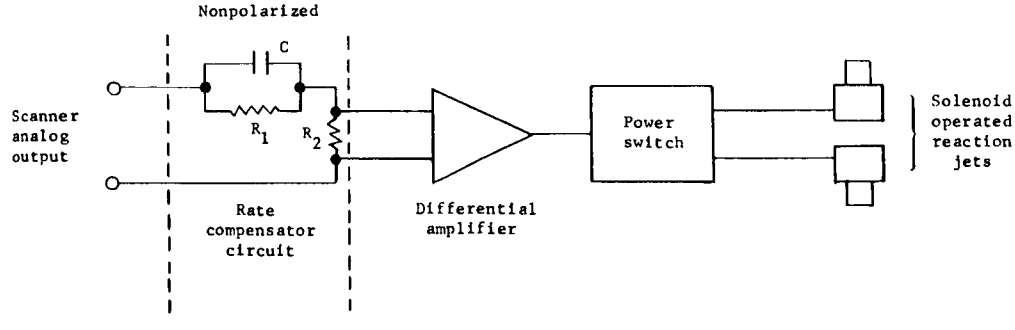

Figure 6.- Block diagram of typical control system for utilizing scanner analog output.

If the TDD pulse is made usable by a maximum-effort control system through the utilization of the pulse-width multiplier, then a pulse-width modulation control system is the end product and this is accomplished without the complicated conversion circuitry normally used. The advantages of this pulse system over the analog system would be reduced limit cycle activity, reduced fuel consumption, and the elimination of dc differential amplifiers in the control system proper (fig. 6).

If an external source of rate information is supplied, this system could also have the important advantage of being extremely simple.

Rejection of unwanted signals.- A significant problem area to be considered in horizon-scanner design is that of discriminating against signals produced by sources other than the target source. For an earth scanner the sun and moon could at times interfere with normal operation. The moon signal can be conveniently rejected by adjusting the triggering threshold of the electronics to operate only on the stronger earth-horizon radiation discontinuity. The sun signal can also be normally dealt with since it is many times that of the earth.

Detection of the stronger sun signal can be accomplished by using zener diodes which allow almost no conduction until their zener voltage is exceeded. If this voltage is exceeded, as occurs when the sun is scanned, the signal is fed through the zener diode to a sun-signal eliminating circuit as shown in figure 7(a) which removes the voltage supply to the TDD and thus prevents the TDD from producing an output for a short time.

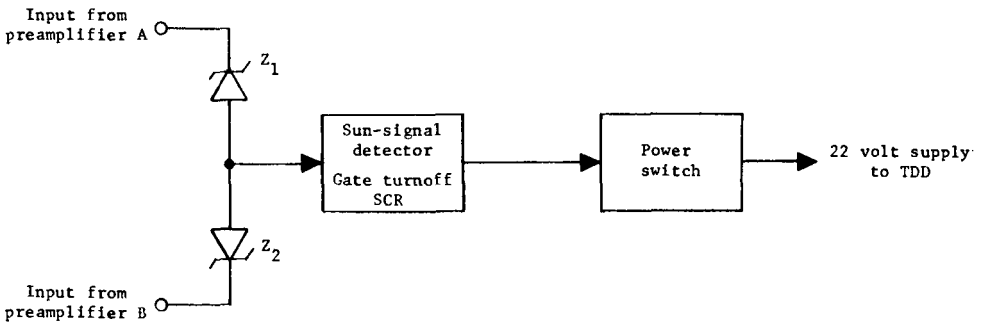

(a) Sun-signal elimination by signal amplitude detection.

Figure 7.- False-signal elimination.

Another method of preventing solar interference would be to use two scanners mounted on the spacecraft so that their fields of view are separated horizontally. The attitude error outputs from the two scanners could be averaged by a simple circuit as shown in figure 7(b). Upon reception of the stronger sun signal by either of the scanners, the output from the other scanner is steered around the averaging circuitry while the output of the scanner viewing the sun is disabled.

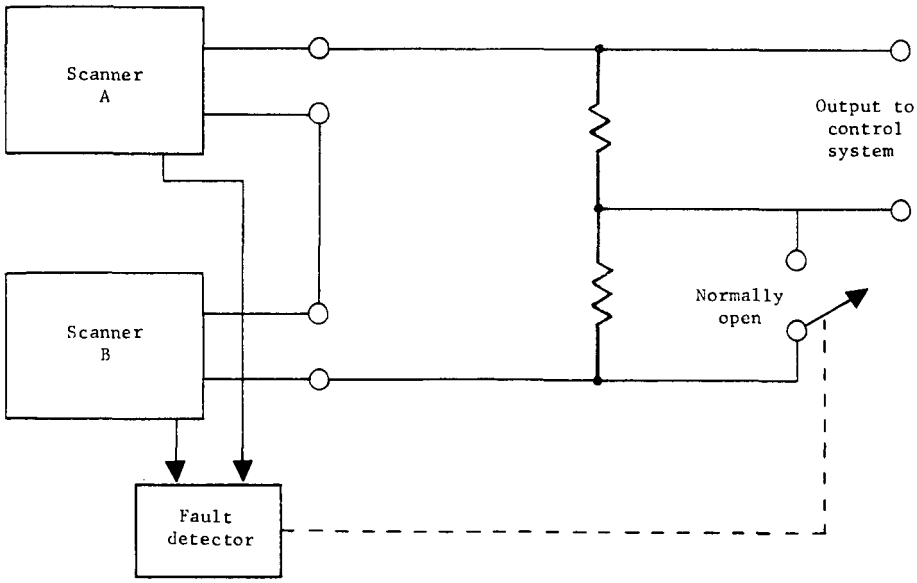

(b) Sun-signal elimination using two scanners.

Figure 7.- Continued.

This technique offers two important byproducts - redundancy and probable increased accuracy. In the event that one scanner ceases to produce an output, through failure or by command, the other scanner can assume the entire responsibility of attitude sensing. Accuracy is increased since the effects of geometric oblateness, high-altitude clouds, and horizon-temperature inconsistencies would tend to be averaged out, particularly if the scanners were positioned on the spacecraft so that separation of their fields of view was maximized (i.e., separation by 45°).

The rejection of earth signals in a moon scanner cannot normally be accomplished by signal-amplitude-discrimination means since the radiation level of the earth falls within the wide range of radiation levels from the moon. However, the relatively small subtended angle of the earth at the moon makes it possible to use angle-discriminating methods.

One such method for use in the proposed scanner might be to modify the scanning mirrors so that the detector fields are split and separated both horizontally and vertically. Horizontal separation would be by a sufficient amount to prevent scanning across the earth by more than one component of the field during any one scan. Vertical separation would be perhaps 3° or 4°. In operation, the first output from the detector would make the circuitry sensitive to a subsequent output by the circuitry modifications shown in figure 7(c).

A somewhat similar earth-discriminating technique would use four additional detectors for producing the additional fields of view without optical modifications. Since, in this case, the two detectors viewing each side of each scanning plane would have to be slightly offset from the focal points of the parabolic reflector segments, it is doubtful that thermistor immersion

techniques would be used. Figure 7(d) shows circuitry modification necessary for the incorporation of this scheme.

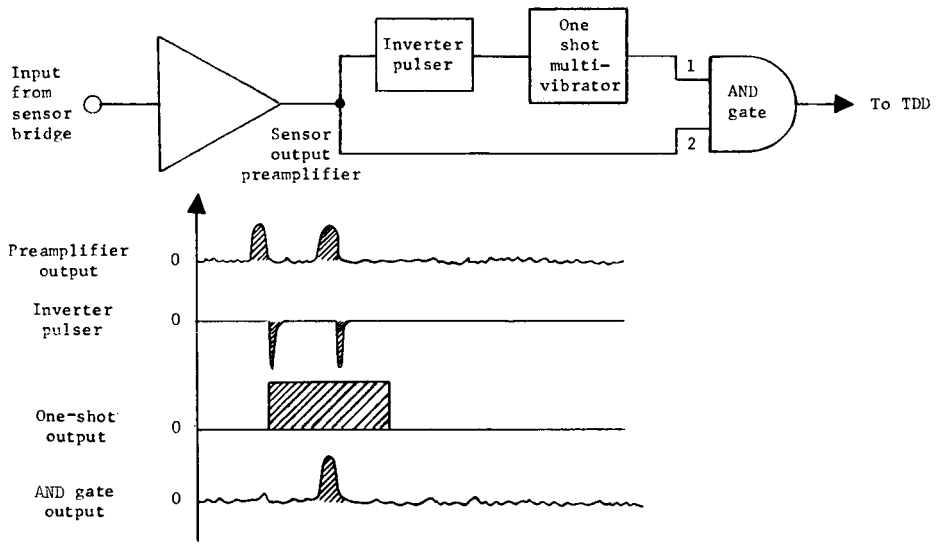

(c) False-signal elimination using split field of view (split mirror).

Figure 7.- Continued.

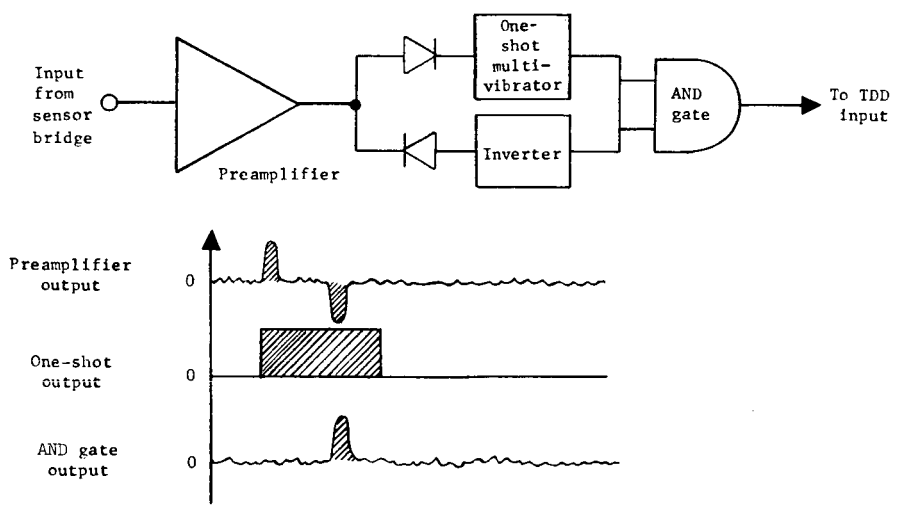

(d) False-signal elimination using split field of view (dual sensors).

Figure 7.- Continued.

A method of greatly reducing the probability of interference from all extraneous radiation sources would be to limit the beginning of the sensitive portion of the scan arc to a point just above the horizon. This operation can be done electronically after orientation is accomplished by delaying the reset pulse. The output from an altitude circuit would be used to compute the proper delay necessary. A block diagram of this circuit is shown in figure 7(e).

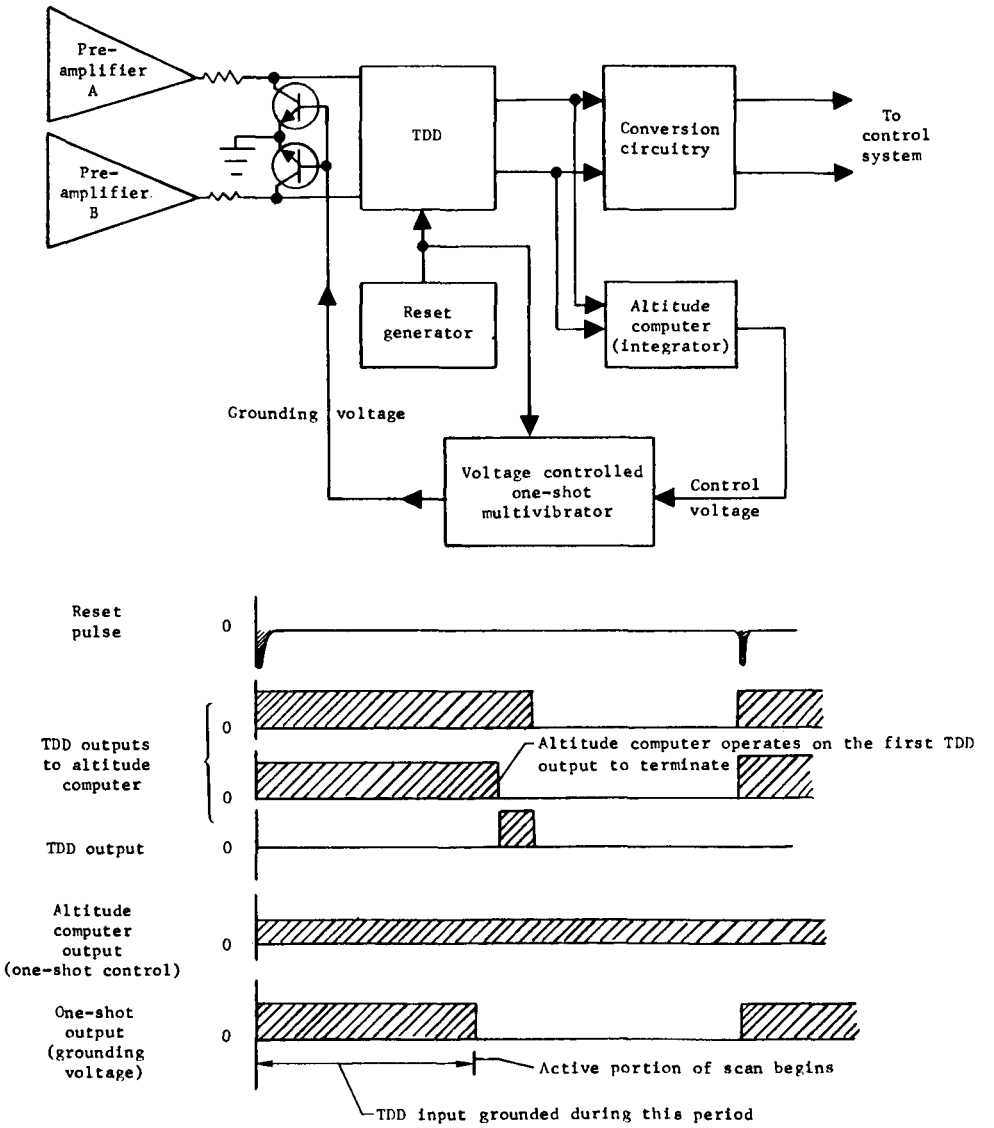

(e) False-signal elimination using restricted field of view.

Figure 7.- Concluded.

Capture Capability

A quantitative estimate of the ability of the scanner to capture a planetary target cannot be made here since capture would be intimately tied in with the spacecraft configuration, inertia, tumble, and roll (about the principal axis of the scanner), and the torque characteristics of the control system. However, the relatively slow sampling rate of the scanner of about 2 samples per second (as compared with 30 or more samples per second for most other scanners) indicates that vehicular rates of no more than perhaps 20 or 30 rpm could be tolerated. If the output of the scanner is to be used for rate indication, far lower sampling rates than this will be required, particularly about the roll axis during capture since at appreciable error angles, roll about the principal axis of the scanner will produce a sinusoidal output from each channel.

The maximum error angle from which an accurate attitude error signal is assured is the field-of-view angle above the scanner's horizontal at which the reset signal is made to occur (30° maximum) plus the horizon-depression angle. However, if the optics are coated to accept a broad spectral bandpass, radiation discontinuities over the surface of the radiating source of most planetary bodies may be expected to trigger the electronics and thus provide usable, though inaccurate, error signals.

Altitude Determination

The signal processing of the scanner is of such a nature that altitude can readily be determined from signals in the circuitry. For example, the average time between the generation of a reset signal and the two horizon crossover signals $\frac{(t_2 - t_1) + (t_3 - t_1)}{2}$, as shown in figure 1, is proportional to altitude.

An analog altitude signal could easily be produced by the use of an integration circuit similar to that used for converting the attitude-error-pulse output from the scanner to an analog output. The integrator would take its input pulse from one side of the TDD to ground. Thus the input pulse would exist for the portion of the scan cycle during which the TDD is not conducting, or from the time the TDD is reset at the beginning of the scan cycle until horizon crossover occurs.

Environmental Considerations

All circuits used in the scanner with the exception of the sensor output amplifiers and the reset generator are inherently stable dc switching circuits and require no special temperature compensation. Slight modifications in the amplifier circuits may be necessary to extend the operating temperature range beyond present values of about 0° C to 70° C. (See the section entitled "Electronic Noise.")

By employing conventional miniaturization techniques (that is, the incorporation of printed circuits, miniature case transistors and SCS's, tantalum capacitors, miniature metal film resistors, etc.), the entire electronics complement, including power regulation devices, can easily be made to conform to the estimated scanner volume of 60 cubic inches. Microminiaturization could be employed if volume, weight, and/or redundancy requirements so dictate.

Radiation damage to the scanner electronics should not be a serious problem. The main concern in this area was possible damage to the thermistor detectors. However, no special precautions against radiation damage would likely be necessary since unpublished results of thermistor radiation tests at inner Van Allen belt levels performed by General Electric showed no significant changes in thermistor characteristics.

PERFORMANCE TESTS

Scanner Test Model

In order to evaluate the performance of the basic scanner design and also to aid in the design and development of the scanner electronics, a test model of the scanner was constructed. The test model uses a mirror drive system that is similar to the one shown in figures 2 and 3 except that it uses a 3000 rpm, 400 cycle motor mounted below the optics to rotate the mirrors at a rate of about 1 revolution per second. Figure 8 shows a picture of the assembled test model; an exploded view is shown in figure 9. Since operation of the scanner in the two attitude sensing planes is identical, the test model was fitted with only two detectors and electronics necessary for processing the detector output in only one plane.

The framework for mounting the various optical, electronic, and mechanical components was machined from aluminum alloy. This frame is in two parts with its separation line lying in the plane of the four rotating mirror shafts. The worm drive gear is machined from stainless steel and the worm gears, which encircle the scanning mirrors, are machined from teflon for low-friction operation. The two germanium lens-immersed thermistor bolometers are 0.15 mm wide by 0.6 mm long. These dimensions, together with the $f/1$ parabolic reflector segments, give the detectors a field of view of approximately 1.5° in the scanning plane by 6° horizontally. The detector time constants are 1.5 ms and 1.7 ms. The germanium lenses are antireflection coated for maximum transmission at 15 microns and have 0.14-inch radii.

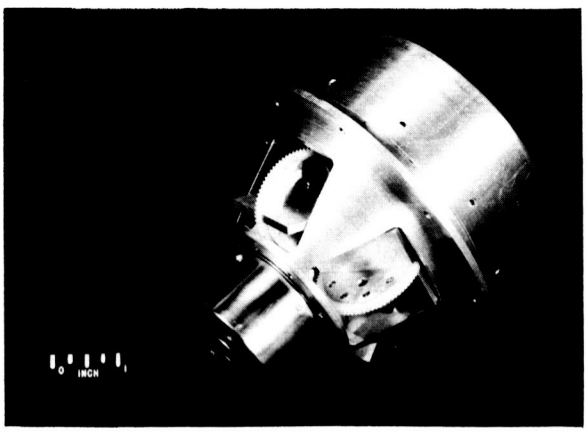

L-60-6509

Figure 8.- Scanner test model.

The flat rotating mirrors are ceramic with their shafts machined from the mirror blanks. Their dimensions are 0.125 inch by 1.5 inches by 1.5 inches and their reflecting surfaces are vacuum-deposited aluminum. The 1-inch by 1.5-inches parabolic reflector segments are cut from pyrex parabolic mirrors and also have vacuum-deposited aluminum surfaces. For easy access, the electronic subcircuits are breadboard versions and use standard-size relatively high-noise germanium transistors. However, all semiconductors in any flight version of the scanner would be high-quality low-noise silicon devices. Total weight of the laboratory test version, including all components for two-axis operation except the electronics, is 25 oz. Miniaturized two-axis electronics would add about 8 oz.

The test model is crude relative to a flight version and thus does not represent either the potential accuracy of the scanner or its minimum power consumption rate. For example, gear backlash is as much as 0.004 inch, which is equivalent to a scan-angle deviation of 0.6°. This excessive backlash was found to be necessary in the test model to avoid gear binding, but could be greatly reduced in a flight version by using a different, more easily machined plastic for the worm gears. Even though some backlash would be necessary in the scanner, it should not contribute substantially to attitude sensing error since the gear driving forces are always in the same direction.

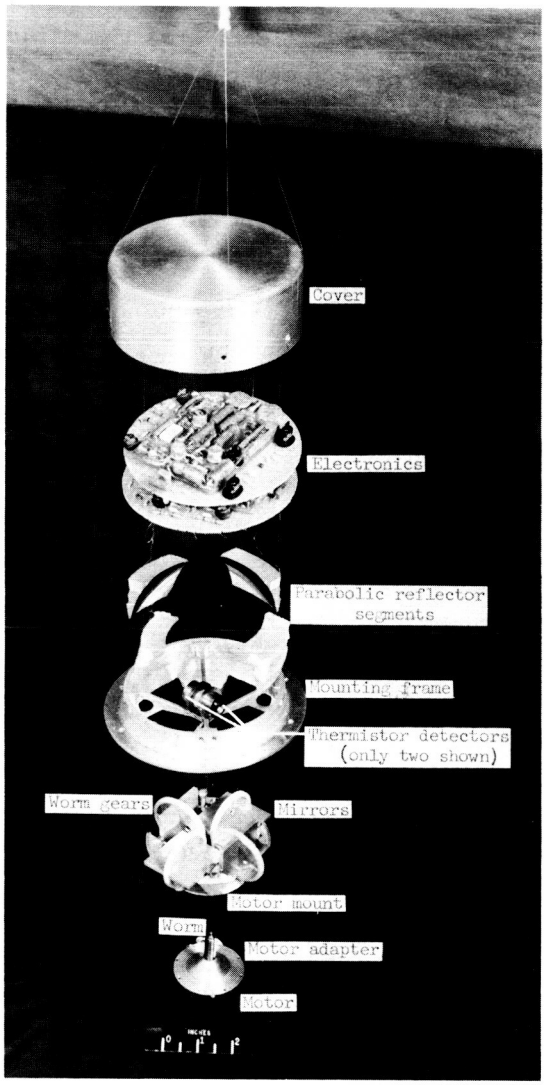

L-60-6511.1

Figure 9.- Exploded view of scanner test model.

Additional attitude sensing errors are produced by imperfections in the optical components and nonexact placement of the detectors at the focal points of the parabolic reflector segments. The optical imperfections consist of nonparallel surfaces on at least one of the doubly faced flat scanning mirrors and unequal reflectivity values of these mirrors. Because of these optical imperfections, alternate pulse outputs from the detectors are shifted by a time-measured duration that is equivalent to about 0.1°. Thus if the scanner is "zeroed in" on a radiating target its output will alternately be shifted by an amount equal to a pointing error of 0.05° on both sides of zero. It is believed that this error can be nearly eliminated in any subsequent model. For this reason and also because it would have been virtually impossible to read consecutive output error signals accurately from the test model on the

oscilloscope, accuracy measurements were made by using alternate output error signals.

A source of error which exists in the test model, but which need not exist in any subsequent model, resulted from having one of the detectors repaired. In repairing the detector its housing had to be modified which required a small

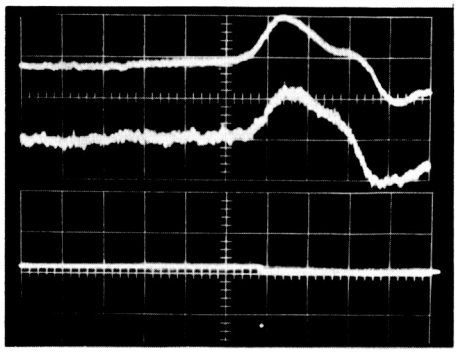

Preamplifier "A" Sensor "A"
(Sensor "A" time constant = 1.5 ms)
2 mV/cm; 5 ms/cm
Preamplifier "B" Sensor "B"
(Sensor "B" time constant = 1.7 ms)

TDD output
20 V/cm; 5 ms/cm

(a) Zero pointing error

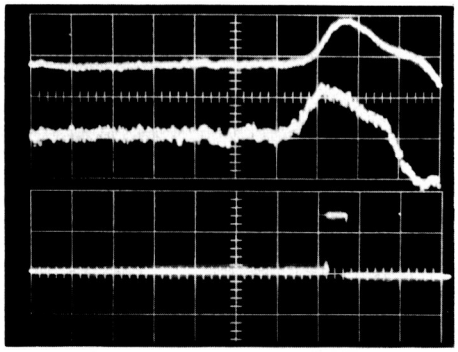

Preamplifier "A" Sensor "A"
2 mV/cm; 5 ms/cm
Preamplifier "B" Sensor "B"

TDD output
20 V/cm; 5 ms/cm

(b) +30 minutes pointing error

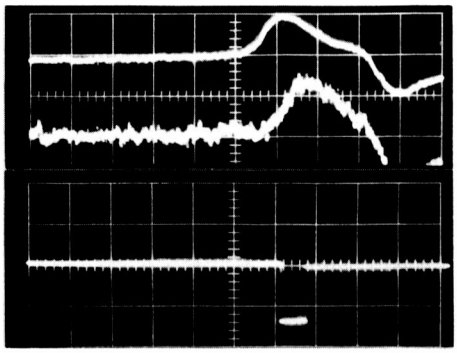

Preamplifier "A" Sensor "A"
2mV/cm; 5ms/cm
Preamplifier "B" Sensor "B"

TDD output
20V/cm; 5ms/cm

(c) -30 minutes pointing error

Figure 10.- Electronics operating waveforms.

displacement of the detector from the focal point of its associated parabolic reflector segment. This displacement, in turn, caused the radiation focused on it to be fuzzy. Still another source of error in the test model was random noise in one of the two thermistor bolometer bridges. This noise, which resulted from mishandling, averaged about 5 percent of the signal produced by the simulated planetary horizon and can be seen in the output of preamplifier B in figure 10. When this noise was superimposed upon the horizon signal, the

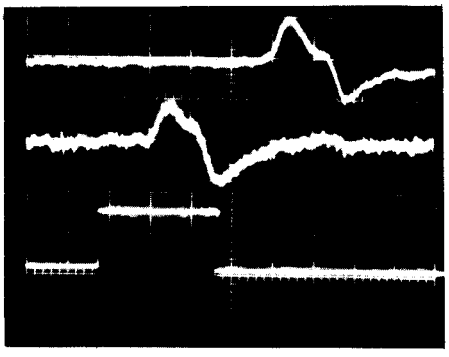

Preamplifier "A" Sensor "A"
2V/cm; 10ms/cm
Preamplifier "B" Sensor "B"

TDD output
20V/cm; 10ms/cm

(d) +5.7 degrees pointing error

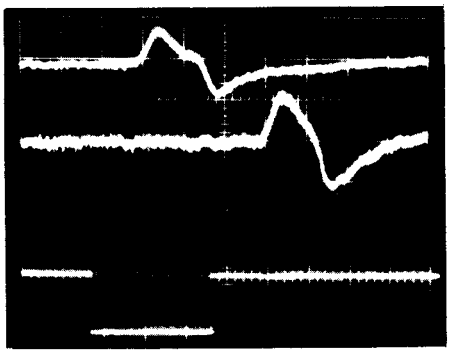

Preamplifier "A" Sensor "A"
2V/cm; 10ms/cm
Preamplifier "B" Sensor "B"

TDD output
20V/cm; 10ms/cm

(e) -5.8 degrees pointing error

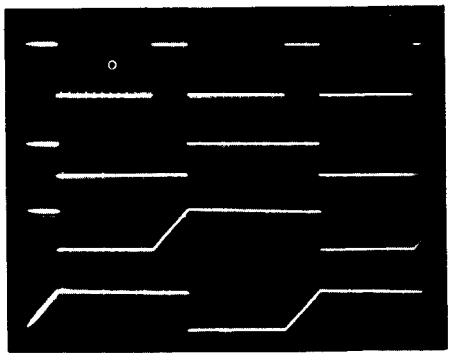

Input pulse 20V/cm
0.2 sec/cm

Multivibrator 10V/cm

Voltage C_1 = 5V/cm
0.2 sec/cm

Voltage C_2 = 5V/cm

(f) Integrator w/forms

Figure 10.- Concluded.

SCS's in this circuit were caused to switch on at slightly different times as the thermistor fields of view scanned across the target edge and produced a false error indication. It should be noted that since figures 10(a) to 10(f) are composite nonsimultaneous photographs of the preamplifier and the TDD outputs, the photographs do not show TDD triggering levels. (Triggering was set to occur at approximately 25 percent of full amplifier output.)

Test Instrumentation

Accuracy tests were conducted with the scanner mounted on the stand shown in figure 11. This stand was fitted with a vernier tilt adjustment and a pointer and scale with which tilt angles could be read to an accuracy of about 0.01°.

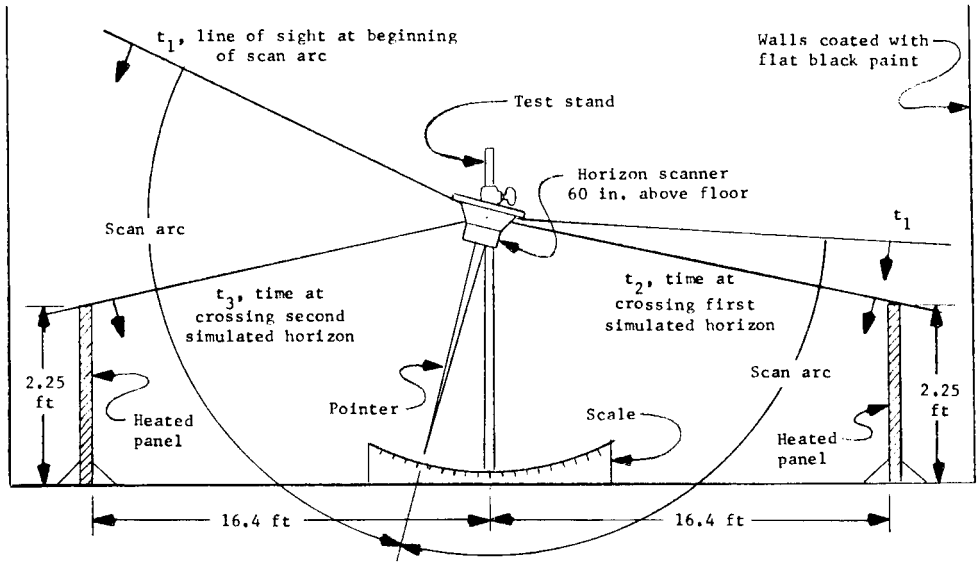

Figure 11.- Setup used in static performance tests.

Capture-rate tests were performed with the scanner mounted on the single-degree-of-freedom air-bearing-supported platform shown in figure 12.

For all accuracy tests the planetary horizons were simulated by a heated panel on each side of the scanner. The panel temperature was adjusted to produce the same radiation power discontinuity at the detectors that would be expected from a 220° K blackbody source, or approximately 23° C warmer than background temperature. Panel temperature was monitored by thermocouples and recorded. Because the panels were only about 16 feet from the scanner, a small amount of optical aberration was produced. This aberration would, of course, be negligible in space.

In order to test the compatibility of the scanner with a typical control system, the test model was mounted on the test platform and its analog output was integrated into the control system as shown in figure 6. The control system

is described in detail in reference 6. The control amplifiers actuated appropriate solenoid reaction jets in response to the rate circuit output.

Attitude Sensing Accuracy

Attitude-sensing-accuracy tests were conducted with the scanner mounted on the test stand (fig. 11). In all these tests zero pointing error was taken as the point where the attitude error indications of the scanner were centered about zero output. It was found that after the scanner output was centered, pulse outputs would not shift by more than $\pm 0.1^{\circ}$. Linearity of the pulse output was found to be within ± 1 percent throughout the attitude-sensitivity range of the scanner. This, then, is the instrument-associated attitude sensing error of the experimental scanner and can be largely attributed to improper handling and construction defects previously discussed. Figure 13(a) shows the pointing error output from the time-difference detector as a function of actual error. The output of the integrator as a function of pointing error is shown in figure 13(b). The integrator output has a ripple component that has fundamental frequency equal to that of the scan rate. This ripple, however, represents less than 2 percent of

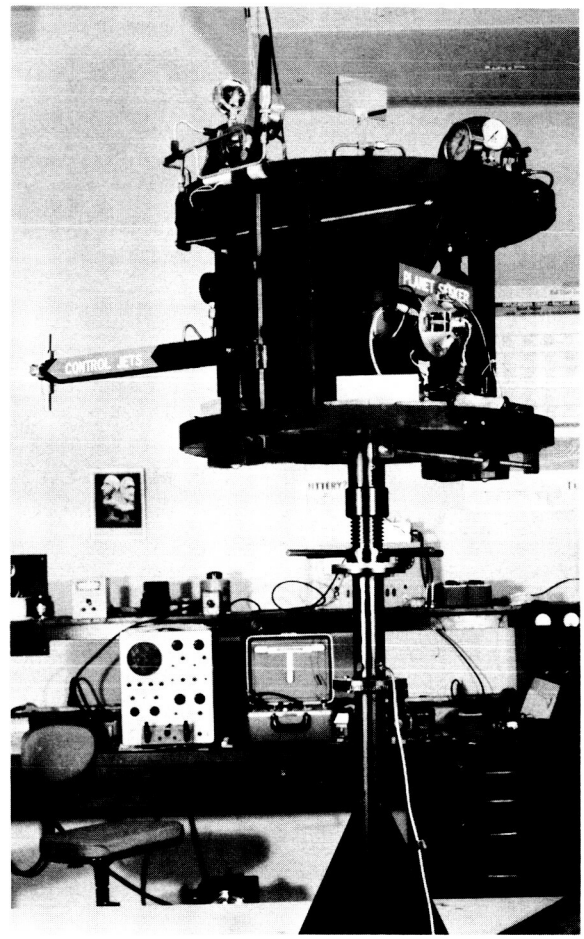

L-64-7326

Figure 12.- Horizon scanner mounted on air bearing.

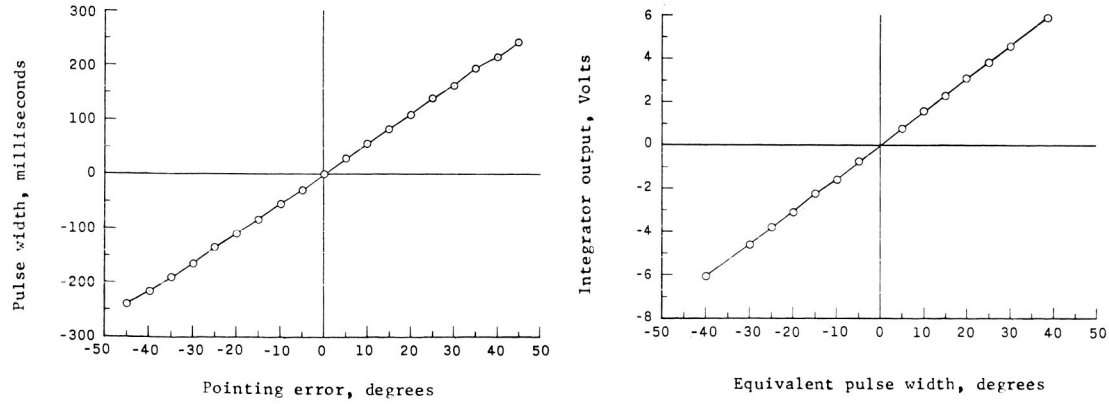

(a) TDD output pulse width as a function of actual pointing error.

(b) Integrator output voltage as a function of equivalent TDD output error pulses.

Figure 13.- Measured attitude error output signals as functions of pointing error.

the output voltage from 1° to 60° error rising to about 3.6 percent at about 0.1° error. The accuracy of the scanner did not decrease appreciably with pointing error through the error range investigated. Figure 10 shows oscilloscope photographs of some of the circuit waveforms appearing in figure 5.

Due to the optical design and constant scanning speed of the scanner the accuracy would be nearly constant throughout its operational altitude range. Therefore, accuracy at only one simulated altitude was investigated.

Altitude Range

An attempt to determine the maximum operational altitude range of the test model scanner was made by decreasing the subtended angle of a heated disk until the scanner ceased to produce reliable attitude signals. This angle was found to be equivalent to an altitude of only about 140,000 miles from the earth due to the fact that the motor on the test model restricted the detector fields of view as they approached the principal axis of the scanner. However, this altitude restriction would not exist in any subsequent model in which the motor mounted below the optics in the experimental scanner would be replaced by a motor mounted above the optics or by the drive system described in appendix A. Thus, the maximum operational altitude would be limited by electronic noise, since the horizon crossover signal would start approaching the electronic noise level as the subtended diameter of the target becomes less than the width of the field of view.

With amplifier gain adjusted to maximum it was found that, in spite of noise in the damaged detector, the test model scanner would operate reliably with the heated-panel temperature adjusted to 3° C above that of the adjacent wall, which was at normal room temperature. This discontinuity corresponds approximately to that which would be detected by the scanner upon crossing the horizon of a planetary source radiating as a blackbody at 125° K. It also corresponds approximately to the discontinuity which would be detected by the scanner at a distance of 660,000 miles from the earth and indicates that a subsequent scanner, in which electronic noise is reduced by the predicted order of magnitude as discussed in the section entitled "Electronic Noise," would operate reliably at a distance of nearly a million miles from the earth and over 100,000 miles from the shaded side of the moon.

Minimum operational altitude would be that at which the radiation discontinuity at the atmospheric horizon becomes so unclearly defined that the detector outputs are insufficient to trigger the electronics.

Performance on Air Bearing

Several tests were performed with the test model mounted on the air-bearing-supported test platform, using both the dc output and pulse outputs of the scanner. The objectives of these tests were to get an indication of (1) the simplicity with which the scanner output could be effectively utilized by a typical control system, (2) the time required for the system to capture the simulated planetary target as a function of different jet pressures and initial

error angles, and (3) the accuracy with which the scanner would hold the test platform after capture.

For tests using the analog dc output of the scanner this signal was integrated into the attitude control system of the test platform as shown in figure 6 and the rate circuit mentioned previously was adjusted to give critical damping and therefore minimum capture time for each test. The test platform was then disoriented with respect to the simulated planetary target and allowed to capture. The times required for capture as a function of control jet pressures and initial pointing error are shown in figure 14. A jet pressure of 27 psi was the maximum permitted by the pressure regulators on the platform. However, the trend toward decreased capture time with increased jet pressure indicates that further reductions in capture time could be obtained.

Steady-state pointing accuracy of the system after capture, as measured by optical means, varied from $\pm 0.15^{\circ}$ at pressures of from about 2 to 5 psi to about $\pm 0.5^{\circ}$ at 27 psi. This increased error with increasing jet pressure was due primarily to the relatively slow attitude sampling rate of the scanner and indicates that a trade-off between scan rate and steady-state accuracy may be necessary if extremely fast capture times are required. If such a trade-off is undesirable a two-mode control system employing high- and low-control torques with corresponding rate circuits could be used. This system would combine fast capture time with a high accuracy capability.

In tests to investigate the probable usefulness of the pulse output of the scanner for spacecraft attitude control, the pulse output was integrated into the control system as shown in figure 15.

The full-wave diode bridge produces a positive pulse for the pulse width multiplier regardless of the polarity of the input pulse. The NPN transistors (Q_1 and Q_2) act as switches that ground the input to either jet depending upon the signal from the integrator.

With a pointing error the time-difference detector gives an output which is fed simultaneously to the pulse-width multiplier and the integrator. The pulse-width multiplier feeds the driving pulse to the control jets and the integrator switches on the correct jet according to the polarity of the time-difference-detector pulse. As pointing error decreases the time-difference-detector pulse width decreases and the integrator output level decreases. If the level decreases at a rate faster than that predetermined by the RC rate circuit, the capacitor causes the voltage to be reversed and the opposite jet is cut on.

In these tests the scanner held the platform to within $\pm 2^{\circ}$ after capture times which were about equal to those for the dc analog output. This relatively large error was the deadband produced by the rate switching circuit used. However, this circuit is in its initial stages of development and by going to lower level switching transistors and increasing the maximum integrator output and saturation angle, it should be possible to reduce the deadband by nearly two orders of magnitude.

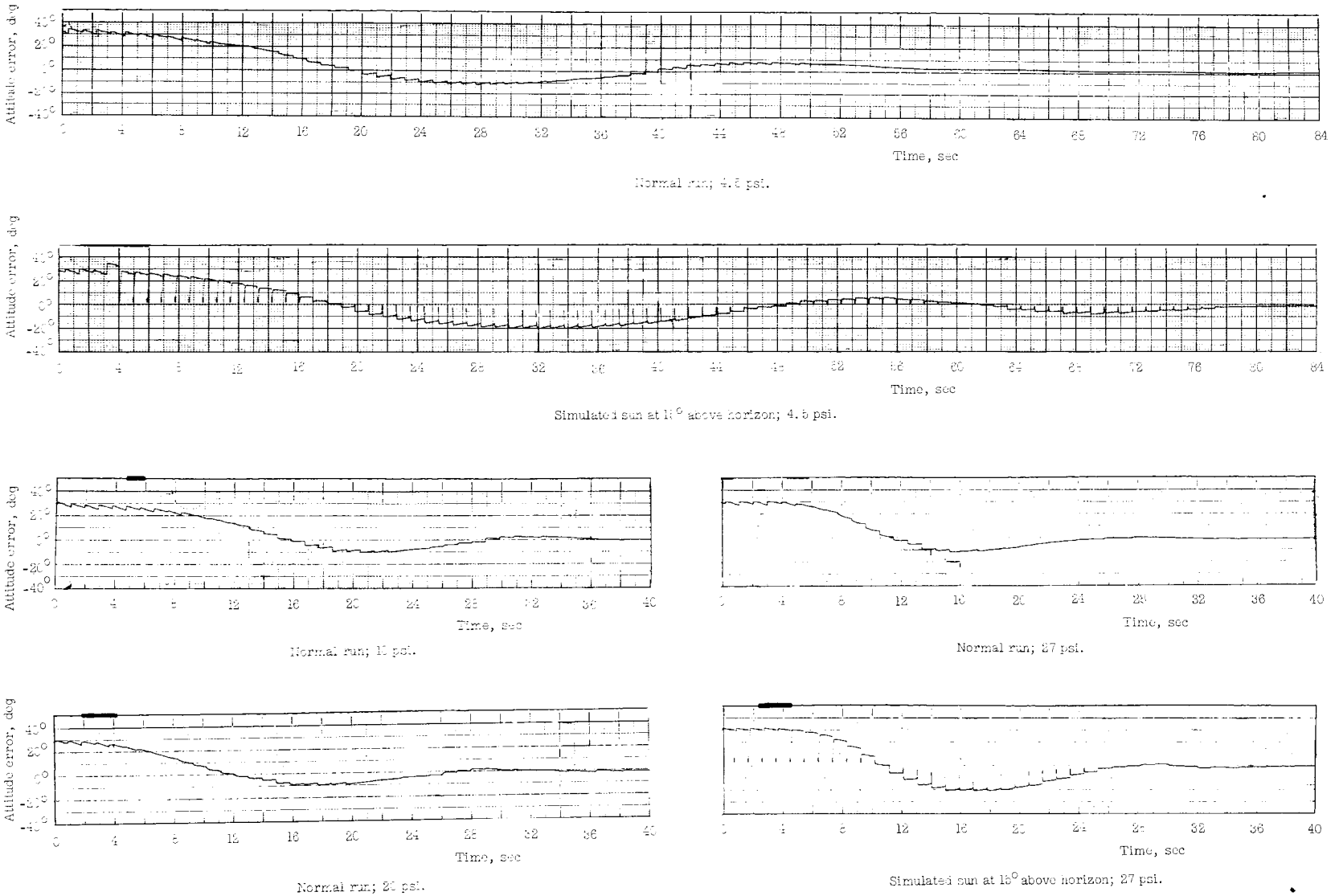

Figure 14.- Recordings of horizon scanner output during capture tests. Voltage scale: 0.1V = 2°.

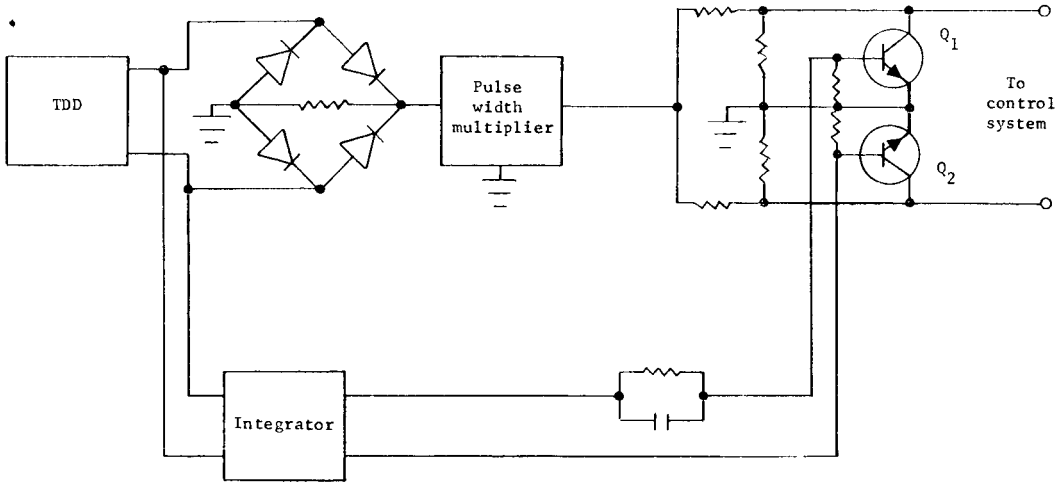

Figure 15.- Rate system used for pulse-width multiplier.

Rejection of Unwanted Signals

Only one of the previously suggested techniques for rejecting signals from extraneous radiation sources was investigated experimentally. This technique was the one using zener diodes to detect the stronger sun signal (fig. 7(a)).

With the test model mounted on the air-bearing platform, a hot soldering iron heat source used to simulate the sun was placed into the field of view at a position about 15° above one horizon simulator. A recording, showing the scanner output during operation of the sun-signal eliminator, appears in figure 14. As can be seen, the output goes to zero where the detector field of view passes over the sun simulator but the output is returned immediately when the horizons are again crossed. Interference with normal operation occurred when the soldering iron was lowered to about 7° above the horizon.

If the interference angle (angle above the horizon) is to be lowered from its present value, using this method of eliminating the sun signal, a detector that has a faster time constant than the one employed must be used.

Power Consumption

Power consumption of the various components of the scanner was measured and is shown in the following table:

	Voltage, V	Current, mA	Power, W
Sensor bridge	-22.5 and +22.5	0.3	0.013
Sensor preamplifiers	+30	10.0	0.300
Time-difference detector	+22	10.0	0.210
Sun-signal eliminator:			
Operating	+30	40.0	1.200
Idling	+30	0.1	0.003
Reset generator	+30	7.0	0.210
Integrator (analog):			
Zero error	+30	14.0	0.420
40° error	+30	30.0	0.900
Drive motor (400 cps)	85	30.0	2.550
Normal total			3.706
Total at 40° error			5.383

In any subsequent model it is recommended that main supply voltages be reduced from 30 volts to 12 volts (except the sensor bias which will remain at about the same value). This voltage reduction will reduce power requirements of each electronic unit to less than half the values shown. Two-axis electronics would therefore consume less total power than the single-axis breadboard electronics. Little redesign would be necessary for this change. Power requirements would also be reduced by the use of either a more efficient drive motor or the drive system discussed in appendix A. Thus, the predicted normal total power requirement of any subsequent two-axis scanner is on the order of 3.0 to 3.5 watts.

Regulation could be provided by a dc-dc converter which would supply detector bias and the two separate (isolated) 12-volt sources required for the TDD and integration circuits. This type of converter is commercially available and can be chosen to be compatible with the main power source of a particular space vehicle.

Electronic Noise

There are only three possible sources of electronic noise in the electronic circuitry of the scanner. The first source is Johnson noise in the detectors themselves and is due to the presence of impurities in the semiconductor material used. This source does not create a problem since its level is far below the horizon crossover signal levels. The magnitude of this noise is unmeasurable without very specialized test equipment. The 1/f noise which

also originates in the detectors is not a problem since the detectors are ac coupled to the electronics.

The third source of noise is in the sensor preamplifiers. Here the main contributors are in the transistors employed. Signal levels from the sensor bridges, resulting from crossing typical radiation discontinuities at the planetary horizons, are on the order of a millivolt or more. With this much signal available, amplification factors of about 2000 are adequate for processing. Gains of this order were easily met by using comparatively noisy germanium devices with no detectable interference. Measured noise, with grounded input, was ±50 millivolts for the preamplifier used in the experimental model. The signal-to-noise ratio of this amplifier, disregarding source noise, with a typical 1-millivolt signal produced by the earth's horizon and a gain setting of 2000 is

$$\frac{\text{Signal}}{\text{Noise}} = \frac{2.000 \text{ volts}}{0.050 \text{ volt}} = 40, \text{ or } 32 \text{ dB}$$

There are many methods which may be employed to reduce the noise level of the sensor preamplifiers. The incorporation of low-noise silicon devices, the use of low supply voltage to the input stage, and the addition of one or more stages of gain to reduce individual amplification levels are three methods that are recommended. It is estimated that noise can easily be reduced by an order of magnitude by using these methods, thereby increasing the signal-to-noise ratio to 400 or 52 dB.

CONCLUDING REMARKS

A horizon scanner for use in determining the attitude of spacecraft relative to the moon and planets has been designed. Although the scanner has moving parts, these parts operate at relatively low speeds and thus would probably not create a serious lifetime limiting factor. On the basis of the considerations discussed and performance tests conducted with an experimental model of the scanner, it is estimated that the proposed scanner would have the following characteristics:

1. Its attitude output signals could exist in either or both pulse and dc analog form which could easily be adjusted in width and amplitude, respectively, to meet the requirements of the mission.

2. It would have a total instrument-associated error of less than 0.1°. Linearity of the pulse output should be within ±1 percent throughout the error sensitivity range of the scanner.

3. Its operational altitude range could extend to nearly 1 million miles from the earth, and over 100,000 miles from the shaded side of the moon.

4. Its total weight, volume, and power requirements would be approximately 3 pounds, 60 $in.^3$, and 3.5 watts, respectively.

5. Capture of a planetary body could be accomplished from relatively large error angles. If the output of the scanner is used for rate, however, near critical damping could only be achieved for low tumble and roll rates.

An electromagnetic drive system discussed in an appendix appears to be feasible for use in the scanner. This system should extend the lifetime of the scanner while also decreasing its weight, volume, and power consumption.

Langley Research Center,
National Aeronautics and Space Administration,
Langley Station, Hampton, Va., May 26, 1965.

APPENDIX A

ALTERNATE MIRROR DRIVE SYSTEM

Although the mirror drive system discussed previously should be capable of operating for longer periods of time in space than other scanners having moving parts, the possibility of incorporating a nonconventional low-friction drive system capable of operating for several years in space was investigated. An electromagnetic drive system appears promising.

The electromagnetic drive system is quite different in operation from that shown in figure 2 although it does not alter the operating principles of the scanner in any way. In the electromagnetic drive system the mirrors are oscillated through arcs of about 60° at a rate of about 4 cps to provide scan arcs of about 120°. The scanning mirrors are faced only on one side and are all in phase. Thus the scan cycles in the two planes are not staggered as they are in the test model scanner and in the drive system shown in figure 2. The electromagnetic drive system consists basically of a solenoid in which the solenoid coil is attached to the scanner framework and the ferrous slug is attached to one of the mirrors as shown in figure 16. The necessary scan-angle phase relationship is maintained by a set of gears which are attached to the mirrors and mesh at the principal axis of the scanner.

The mirrors have a rest position determined by three permanent magnets. Two magnets are mounted to a gear sector and one is fixed to the scanner frame. The three magnets are positioned in such a manner that the fields of the two mirror-mounted magnets oppose the field of the fixed magnet and thus tend to position the mirrors at some point between their scan-arc limits. When the solenoid is pulsed, the ferrous slug is pulled into the coil and the lower, mirror-mounted magnet will be moved closer to the fixed magnet. Equilibrium of the forces exerted by the magnet fields is now overbalanced and a net force is exerted on the lower mirror-mounted magnet opposing the force of the solenoid. When the current through the coil is stopped, the mirror will be forced by the opposing magnetic fields back through the mirror rest position. The upper mirror-mounted magnet will now exert a force on the fixed magnet and return the mirror to a point at which the solenoid will act upon it, and so on. By varying the width and frequency of the pulses to the solenoid

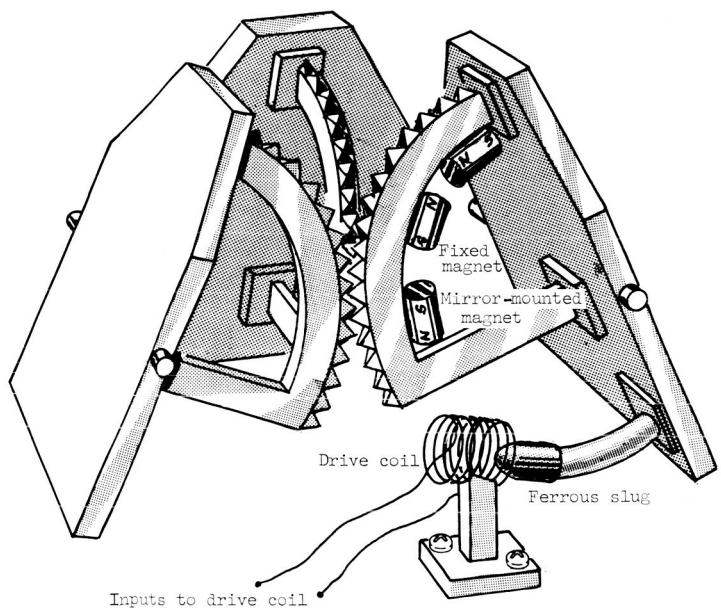

Figure 16.- Alternate mirror drive system.

and the size of the magnets, the mirrors can be made to oscillate at different frequencies and amplitudes.

The electronics associated with this drive system consists of a specially designed astable multivibrator in which period, on-time, and off-time are adjustable. The on-time pulse is amplified to drive the actuating solenoid.

Torsion bars or flexure pivots might be used in place of magnets in the electromagnetic drive system, although some difficulty would be encountered in attaching the torsion bars to the mirrors in such a way that they could be contained entirely within the scanner. This could be done, however, by having the torsion bars pass through the mirrors along the rotational axes of the mirrors with one end of each bar attached to one side of the mirror and the opposite end attached to the scanner framework.

Constancy of mirror rotational velocity throughout a major portion of the scan arc can be approached by shaping the driving pulse, using feedback to the pulse-producing circuitry from a simple auxiliary rate pickup coil and slug.

A simple test model of the electromagnetic drive system was constructed and tested. In the test model (fig. 17) the gears, with moments of inertia chosen to roughly equal those of the mirrors and gearing system of an operational scanner, were oscillated at 4 cps through arcs of about 45° at an average power-dissipation rate of about 0.8 watt by using magnets to oppose solenoid forces. Power consumption could undoubtedly be reduced in a system such as that shown in figure 16 where more efficient coils and a much reduced air gap between the coil and the slugs would be used. By careful selection and placement of the magnets the scan can be extended to 60° or more.

To evaluate the operation of the system with torsion bars the magnets were removed, torsion bars were attached to the gear shafts of the electromagnetic-drive-system test model, and driving signals were applied to the solenoid as before. The gears were oscillated through arcs of about 60° at an average power consumption rate of about 1 watt. With both the magnet and the torsion-bar system, it was found that the frequency of the pulses applied to the solenoid coil was not critical and could be changed by a factor of 2 about the frequency at which maximum scan arc occurred with a decrease in scan arc of only 10° to 15°.

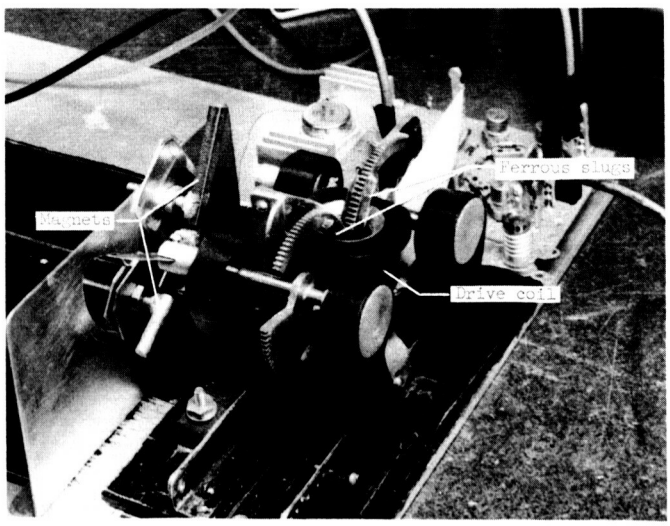

L-64-5373.1

Figure 17.- Alternate drive system test model.

APPENDIX B

DETAILS OF EXPERIMENTAL SCANNER ELECTRONICS

Basic Scanner Electronics

Figure 18 shows in schematic form the basic scanner electronics. The pulses from the bolometer bridges, after sufficient amplication by the sensor preamplifiers, are applied to the TDD gate circuits via the input diodes D_1, D_2, D_3, and D_4. These diodes assure that negative-going pulses from the preamplifiers do not prematurely turn off the SCS's.

The reset pulse is amplified by the Darlington amplifier and used to fire S_3 to provide a negative-going square-wave pulse with a leading edge of less than 2 microseconds. This square-wave pulse is differentiated by C_3 and R_5 and the positive portion is shorted by D_7. This negative pulse is also fed to the sun-signal eliminator for turnoff in the event the sun is in such a position that normal turnoff is not affected.

The triggering thresholds of the TDD inputs are about 0.55 volt and gain controls are provided in the preamplifiers for adjusting the switching level.

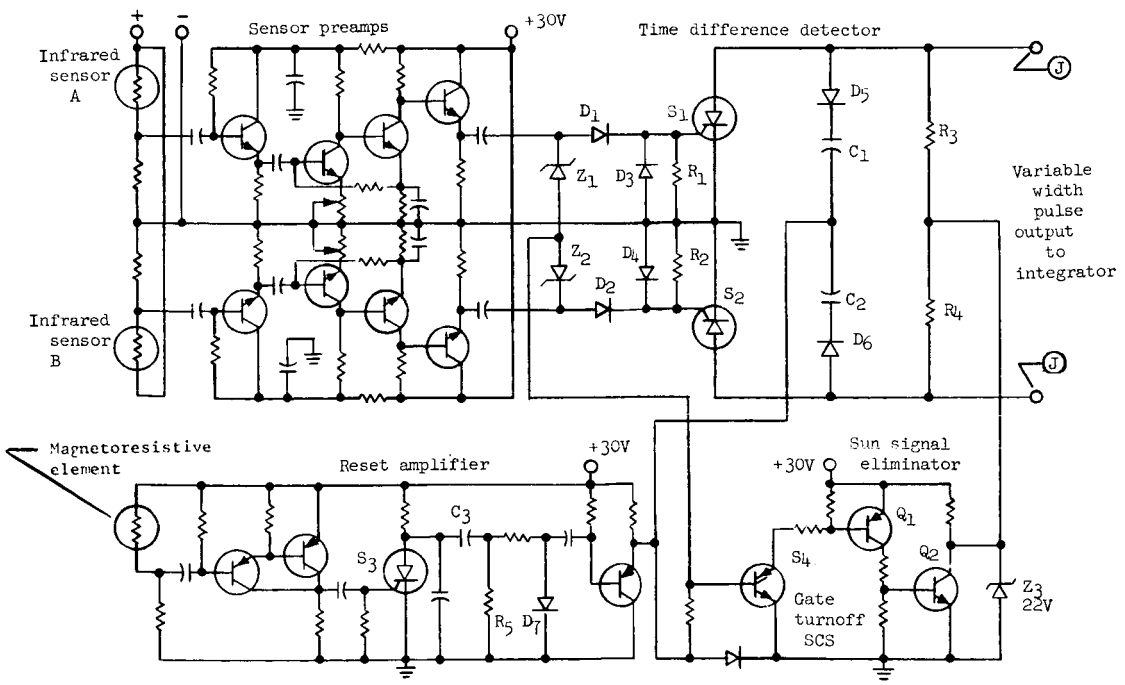

Figure 18.- Horizon scanner electronics schematic.

APPENDIX B

Sun-Signal Eliminator

Sun signals processed by the preamplifiers are of sufficient magnitude to exceed the zener voltage of Z_1 and Z_2 and are therefore fed to the gate of S_4 (gate turnoff SCS). When S_4 fires, Q_1 and Q_2 are biased into conduction, thereby removing the 22-volt supply to the TDD. When the supply voltage is removed, the TDD SCS's are simultaneously cut off, if they had been triggered, thereby halting any output in this axis until the supply voltage is returned. The TDD is therefore held insensitive to all incoming signals during operation of the sun-signal-elimination circuitry. The trailing edge of the sun signal, being negative due to differentiation in the sensor preamplifiers, cuts off S_4, thus returning the 22-volt supply to the TDD, allowing normal operation during the remainder of the scan. Since one circuit of this type is used for each axis, normal operation of the axis not viewing the sun is unaffected.

Conversion Circuitry

Analog circuit.- The analog circuit for converting the TDD pulse output to a dc voltage is shown in figure 19. In this circuit two capacitors C_1 and C_2 are alternately charged and read. While one capacitor is being charged, the other is being read by a high input impedance circuit. The alternating charge-and-read process is actuated by the bistable multivibrator formed by Q_4 and Q_5

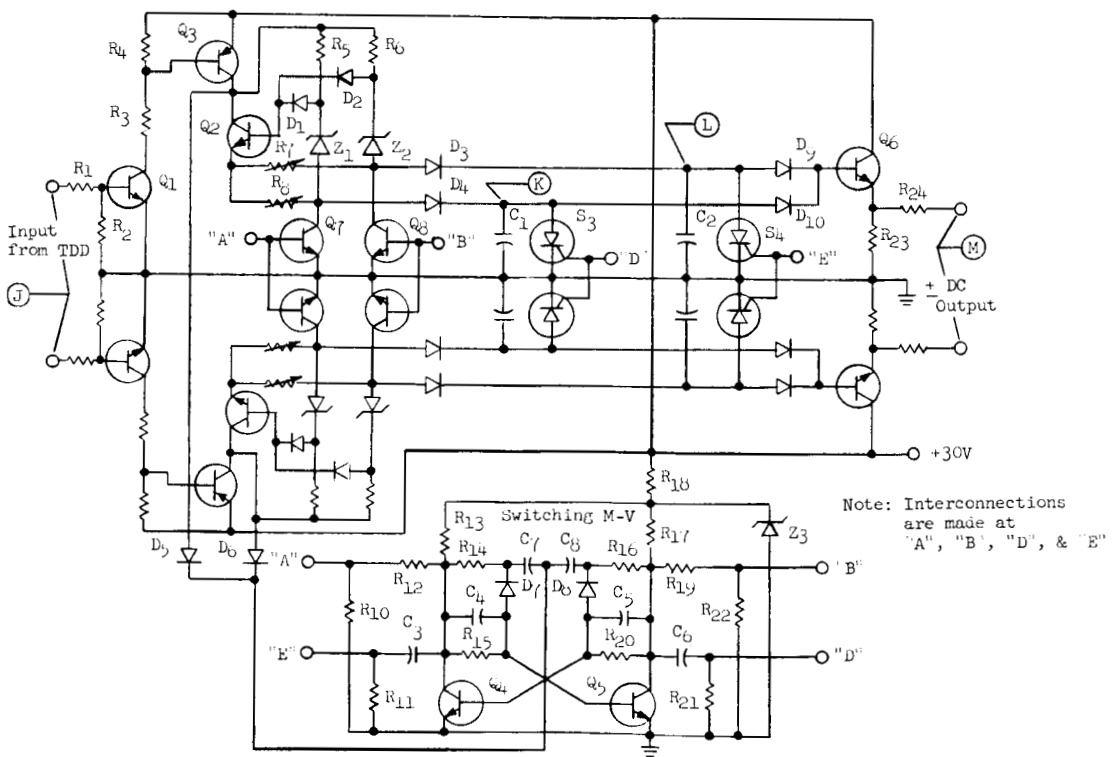

Figure 19.- Schematic of integrator used in test model scanner.

which is triggered by the trailing edge of the error pulse. The input pulse is alternately steered to the proper capacitor by transistors Q_7 and Q_8 which are biased into conduction by the multivibrator. This steering method merely shunts the error pulse to ground of the capacitor which is being read. At the end of each pulse, the capacitor which is next to be charged is unloaded of its previous charge by a shunted SCS which is also triggered by the multivibrator.

Capacitors C_1 and C_2 are charged by the constant-current charge circuit formed by Q_2, R_7, R_8, D_1, D_2, Z_1, and Z_2. Resistors R_5 and R_6 are zener bias resistors. This circuit is responsible for the linear relationship between the input pulse width and the output voltage. A method for calculating charge parameters is given in figure 20. This figure also shows the method for calculating the maximum output voltage for which essentially linear operation is obtained. Adjustment of the saturation angle discussed in section entitled "Conversion Circuitry" is made with R_7 and R_8 (fig. 19). If desired, two or more fixed values of resistance for R_7 and R_8 could be switched in to provide steeper slopes about small error angles.

The diodes D_3 and D_4 prevent the capacitors C_1 and C_2 (fig. 19) from discharging through the charge circuit. Transistors Q_1 and Q_3 form an impedance buffer to the TDD and saturate when the input pulse reaches 1 volt, thereby making the integrator insensitive to supply-voltage variations. High-impedance readout (500 kΩ) is provided by Q_6 through the diodes D_9 and D_{10} which are connected in a "greater than, OR" configuration.

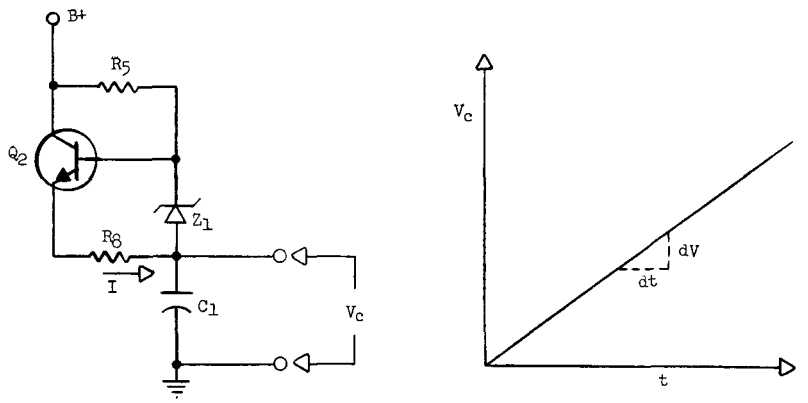

Circuit showing necessary components of figure 19 for calculating charge parameters

The analog integrator consists of two of the previously described circuits connected in a differential configuration employing a common multivibrator. By redesigning this multivibrator to use diode switching for steering the input pulse, steering transistors Q_7

$$V_C = \frac{1}{C}\int i\,dt$$

$$\frac{dV_C}{dt} = \frac{I}{C} = \frac{V_{Z_1}}{C(R_8)}$$

$$C(R_8) = \frac{V_C}{\frac{dV_C}{dt}}$$

Where
C = Capacitance of C_1
i = Instantaneous capacitor current
I = Constant capacitor current

Essentially linear operation is obtained when

$$V_{C_1} = V_{B+} - 2V_{Z_1}$$

Figure 20.- Charge parameter calculation.

and Q_8 can be eliminated; this elimination results in a total saving of four transistors per axis.

A further simplification could also result if a linear output with respect to input pulse width is not required. This simplification would eliminate the constant-current charge path mentioned previously which consists of a total of four transistors and their associated components per axis.

Pulse circuit.- The circuit diagram for the pulse conversion circuit is shown in figure 21. The multiplying circuit consists of Q_1, C, and Q_2. Resistor R_2 serves as the charge path for C and Q_1 and R_3 serves as the discharge path. Zener diode Z_2 determines the magnitude of the voltage that C is charged to, and Z_3 which is the same value as Z_2 holds Q_2 cut off when C is charged to its regulated voltage.

With B+ applied to the circuit and no signal at the input, C_1 is charged to the zener voltage of Z_2 and all transistors are cut off. When a square-wave pulse is applied to the input terminal at time t_1, Q_1 conducts, and C begins to discharge through R_3 via Q_1. When C discharges, Q_2 is biased into conduction

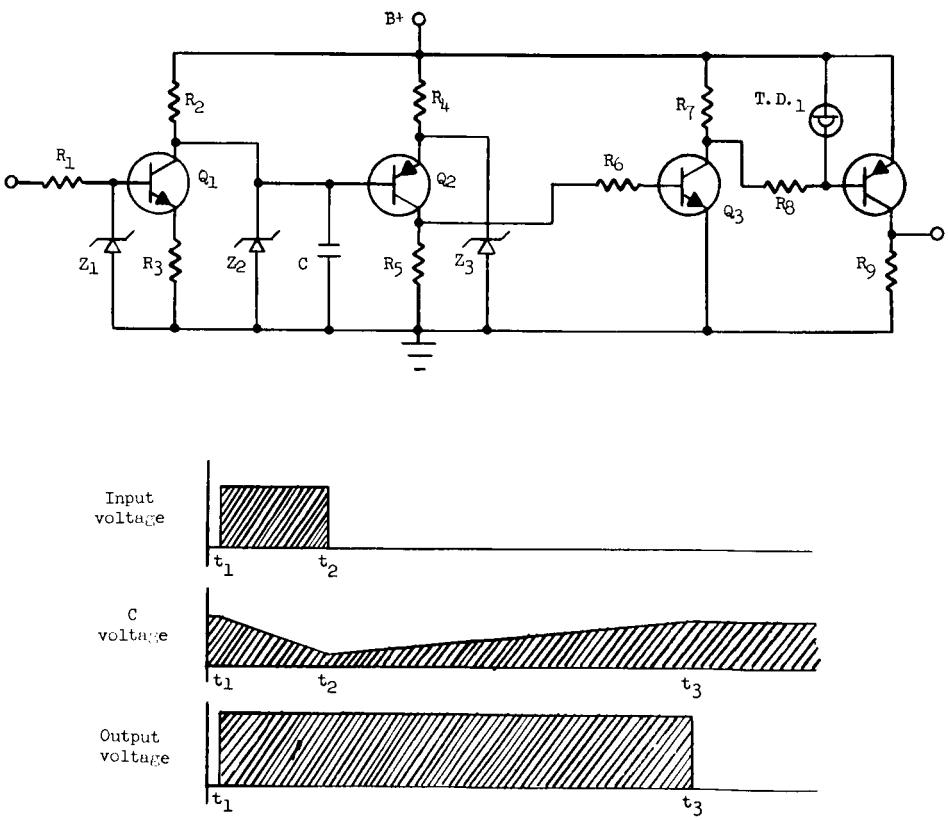

Figure 21.- Pulse width multiplier.

which increases the voltage crop across load resistor R_5. Transistor Q_3 amplifies this increase and switches on tunnel diode TD_1 which in turn switches on Q_4. When the input pulse terminates, at some time t_2, Q_1 is cut off, causing C to charge again through R_2. When C returns to its regulated voltage, the forward bias on Q_2 is removed and conduction ceases. This sequence causes Q_3 to cut off which in turn cuts Q_4 off. Figure 21 shows the relationship between the input pulse, the capacitor voltage, and the output pulse. The multiplication factor of the circuit is

$$\frac{t_3 - t_1}{t_2 - t_1}$$

This factor can be changed by varying R_2. If the input pulse is of sufficient duration to completely discharge C, then the device no longer multiplies the pulse by a constant but merely adds a fixed amount to the pulse as the width increases.

REFERENCES

1. Hatcher, Norman M.; and Germann, Ernst F., Jr.: Study of a Proposed Infrared Horizon Scanner for Use in Space-Orientation Control Systems. NASA TN D-1005, 1962.

2. DeWaard, Russell; and Wormser, Eric M.: Thermistor Infrared Detectors. Pt. 1 - Properties and Developments. NAVORD Rept. 5495, Apr. 30, 1958.

3. Young, W. C.; Clauss, F. J.; and Drake, S. P.: Lubrication of Ball Bearings for Space Applications. ASLE Trans., vol. 6, no. 3, July 1963, pp. 178-191.

4. Podlaseck, S.; and Suhorsky, J.: The Stability of Organic Materials in Vacuum. Ann. Tech. Meeting Proc., Inst. Environ. Sci., 1963, pp. 593-603.

5. Savant, C. J., Jr.: Basic Feedback Control System Design. McGraw-Hill Book Co., Inc., c.1958, p. 179.

6. Fontana, Anthony; Maynard, Julian D.; Brumfield, Marcus L.; and Parker, Otis J.: Flight Investigation of a Solar Orientation Control System for Spacecraft. NASA TM X-944, 1964.

NASA-Langley, 1965 L-4255

"The aeronautical and space activities of the United States shall be conducted so as to contribute . . . to the expansion of human knowledge of phenomena in the atmosphere and space. The Administration shall provide for the widest practicable and appropriate dissemination of information concerning its activities and the results thereof."

—NATIONAL AERONAUTICS AND SPACE ACT OF 1958

NASA SCIENTIFIC AND TECHNICAL PUBLICATIONS

TECHNICAL REPORTS: Scientific and technical information considered important, complete, and a lasting contribution to existing knowledge.

TECHNICAL NOTES: Information less broad in scope but nevertheless of importance as a contribution to existing knowledge.

TECHNICAL MEMORANDUMS: Information receiving limited distribution because of preliminary data, security classification, or other reasons.

CONTRACTOR REPORTS: Technical information generated in connection with a NASA contract or grant and released under NASA auspices.

TECHNICAL TRANSLATIONS: Information published in a foreign language considered to merit NASA distribution in English.

TECHNICAL REPRINTS: Information derived from NASA activities and initially published in the form of journal articles.

SPECIAL PUBLICATIONS: Information derived from or of value to NASA activities but not necessarily reporting the results of individual NASA-programmed scientific efforts. Publications include conference proceedings, monographs, data compilations, handbooks, sourcebooks, and special bibliographies.

Details on the availability of these publications may be obtained from:

SCIENTIFIC AND TECHNICAL INFORMATION DIVISION

NATIONAL AERONAUTICS AND SPACE ADMINISTRATION

Washington, D.C. 20546